

PRECISION INSTRUMENT FOR CHARACTERIZING CONTRACTION AND EXTENSION OF NITINOL WIRE

Sumanth Chikkamaranahalli and R. Ryan Vallance

Precision Systems Laboratory, University of Kentucky, Lexington, KY

Osamah A. Rawashdeh and James E. Lumpp

Embedded Systems Laboratory, University of Kentucky, Lexington, KY

Bruce L. Walcott

Control Systems Laboratory, University of Kentucky, Lexington, KY

Abstract

A large number of commercial applications could benefit from the properties of shape memory alloy (SMA) used in bias-spring actuators. These actuators often use nitinol wires that contract when heated above their transformation temperatures. During cooling, the wire relaxes and is elongated by a bias-spring. In this paper, we describe the conceptual and detailed design of a precision instrument to characterize the transient and steady-state contraction and relaxation of nitinol wires. Additional analyses of thermal and structural compliance conducted during the detailed design are presented. A variety of performance metrics such as the force, displacement, current and voltage can be determined using this instrument.

Keywords: Nitinol, Shape Memory Alloy, Bias-spring actuators, Instrument Design, Uncertainty

Introduction

Nickel Titanium (NiTi), commonly known as Nitinol, is a Shape Memory Alloy (SMA) that returns to a previously defined shape or size when subjected to appropriate thermal procedures [1]. At low temperatures, SMAs can be plastically deformed like other metal alloys, but this deformation can be recovered by subsequently increasing its temperature. This is known as the shape memory effect. The mechanism of this recovery is the transformation from a martensite phase to the parent austenite phase [2].

An important application of shape memory alloys is in actuators where repeated shape, geometry, or positions are required [3]. The important performance attributes in an SMA actuator are the amount of force and displacement produced as the alloy is thermally cycled. Fig 1 illustrates a typical cycle for a SMA actuator that consists of five time periods. During Periods 1, 3, and 5, the actuator is in a nearly steady-state or static condition. The SMA is heated during Period 2 producing a transient displacement when the wire contracts. During

Period 4, the SMA wire cools and elongates to its original length. The response is plotted using a log time scale because the actuation period occurs quickly compared to the cooling period.

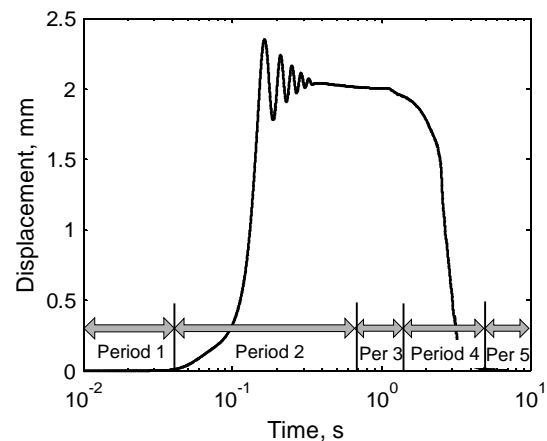


Fig 1: Transient Response of a NiTi Wire

This paper describes the conceptual and detailed design of a new instrument [4] for characterizing the response of NiTi wires. The material being tested is Flexinol™ wire of diameters 0.038 mm, 0.051 mm, 0.102 mm and 0.152 mm and various lengths. The material composition of the Flexinol™ wire is Ni (53%

by weight), Ti (Balance) and impurities (less than 0.03%). The contraction and the extension temperature under 100 MPa stress is $70^{\circ}\text{C} \pm 15^{\circ}\text{C}$ and $50^{\circ}\text{C} \pm 15^{\circ}\text{C}$ respectively [5].

Conceptual Design of the Instrument

The instrument employs a damped, spring-mass system supported by a linear bearing as illustrated in Fig 2. A single NiTi wire is attached between a translating mass and a force gage. A tension spring is attached between the mass and a micrometer so that extending or retracting the micrometer adjusts the preload force in the NiTi wire. The actuation cycle is initiated by resistively heating the NiTi wire by supplying a voltage, $V(t)$, across the NiTi wire. The current, $I(t)$, depends upon the resistance of the NiTi wire.

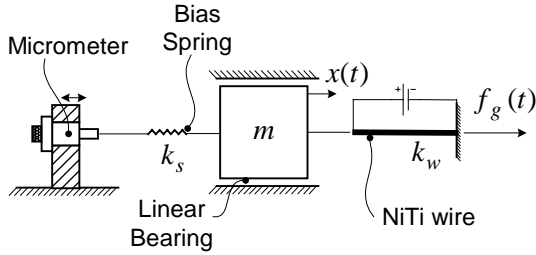


Fig 2: Conceptual Design

Idealized free-body diagrams of the mass during the five static and transient time periods are illustrated in Fig 3. Although the spring stiffness, k_s , remains nearly constant, the wire stiffness, k_w , and damping, c , likely vary with time since the NiTi's properties change with temperature.

Period-1 represents the state of the wire before actuation. The initial force exerted by the spring, iF_s , equals the product of the spring stiffness, k_s , and preload position, x_p . Similarly, the initial force exerted by the NiTi wire, iF_w , equals the product of the initial wire stiffness, ${}^i k_w$, and x_p . As shown in Eq (1), these forces equal the preload force measured by the gage, F_p , and set with the micrometer.

$$F_p = {}^iF_s = k_s x_p = {}^iF_w = {}^i k_w x_p \quad (1)$$

Period-2 represents the transient state of the wire during contraction of the wire. The wire generates an actuation force, ${}^cF_a(t)$, that causes the mass to displace by $x_c(t)$. The wire stiffness during contraction, ${}^c k_w$, and damping, ${}^c c$, likely vary as the material transitions from martensite to austenite. The equation of motion for Period 2 is then given in Eq (2).

$${}^cF_a(t) = m\ddot{x}_c(t) + {}^c c(t)\dot{x}_c(t) + [k_s + {}^c k_w(t)]x_c(t) \quad (2)$$

Period-3 represents the static actuated state of the wire when the mass is held in position by the contracted wire. During this period, the free-body diagram reveals that the product of k_s and actuated displacement, x_a , equals the sum of the steady-state actuator force, ${}^{ss}F_a$, and the product of wire stiffness upon actuation, ${}^a k_w$, and x_a .

$$k_s x_a = {}^a k_w x_a + {}^{ss}F_a \quad (3)$$

Period-4 represents the transient state of the wire as it cools and elongates to its original length. The actuation force during extension, ${}^eF_a(t)$, decreases, and displacement, $x_e(t)$, results. Again, the damping and wire stiffness will likely vary with time, so that the equation of motion for Period 4 is given by Eq (4).

$${}^eF_a(t) = m\ddot{x}_e(t) + {}^e c(t)\dot{x}_e(t) + [k_s + {}^e k_w(t)]x_e(t) \quad (4)$$

Period-5 represents the static or steady-state of the NiTi wire after the actuation cycle. During this state, the mass returns to its initial position. The final force exerted by the spring, fF_s , equals the product of spring stiffness, k_s and the final position of the mass, x_f . Similarly, the final force exerted by the NiTi wire, fF_w , equals the product of the final wire stiffness, ${}^f k_w$, and x_f . As shown in Eq (5), these two forces are equal.

$${}^fF_s = k_s x_f = {}^f k_w x_f = {}^fF_w \quad (5)$$

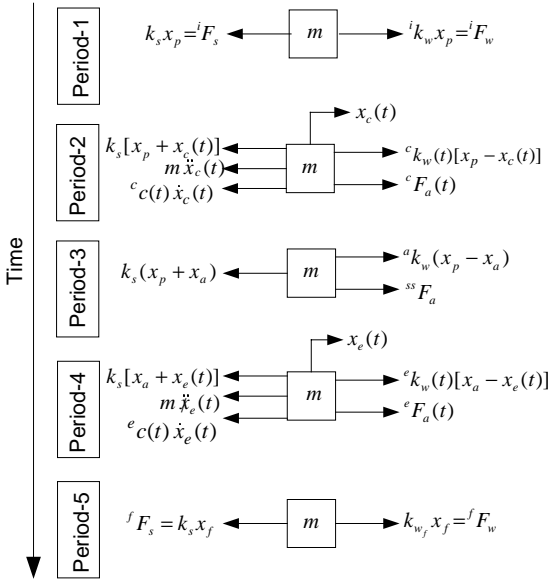


Fig 3: Idealized Static and Dynamic Periods During Characterization of NiTi Wire

Detailed Design of the Instrument

The entire setup is mounted on a base plate machined from cast iron (CI –30) as shown in Fig 4. The instrument consists of a linear motion stage supported by a porous-graphite air bearing (NewWay, S40400305). The bearing consists of a housing and an aluminum guide bar. An important advantage offered by air bearings is its low static and dynamic friction. This is vital since friction force would introduce significant uncertainty in the measurement of contraction

forces. Nitinol wires of various lengths and diameters can be attached to one end of the linear motion stage by adjusting the position of the load cell mount.

The other end of the nitinol wire is attached to a stationary load cell (Sensotec, Model 31a, sensitive to tensile forces between 0- 445.0797N (0-100 lb) with a non linearity of $\pm 0.2\%$ full scale) A tension spring connects to the opposite end of the guide bar to establish a preload force on the nitinol wire. The preload and length of the tension spring are adjusted using a micrometer, (Starrett, No.261L, with a displacement range of 0-12.7mm). This arrangement of the spring and the wire places the forces near the bearing’s center of stiffness.

The displacement of the guide bar during the contraction and relaxation of the nitinol wire is measured using a Linear Variable Differential Transformer (LVDT). (Sentec, Model DCFS3/4 with a nominal linear range of 19 mm (0.76 inches), resolution of 0.001% full scale, and a non-linearity of 0.2%) housed within the air-bearing shaft. The output of the LVDT is a $\pm X$ V analog signal.

The transducer core is fastened to the end plate (Al-6061) by means of a threaded stud. The transducer body is held in its position by a clamp (Al-7075). This arrangement illustrated in Fig 5 places the LVDT in the center of stiffness of the air bearing and minimizes Abbe errors.

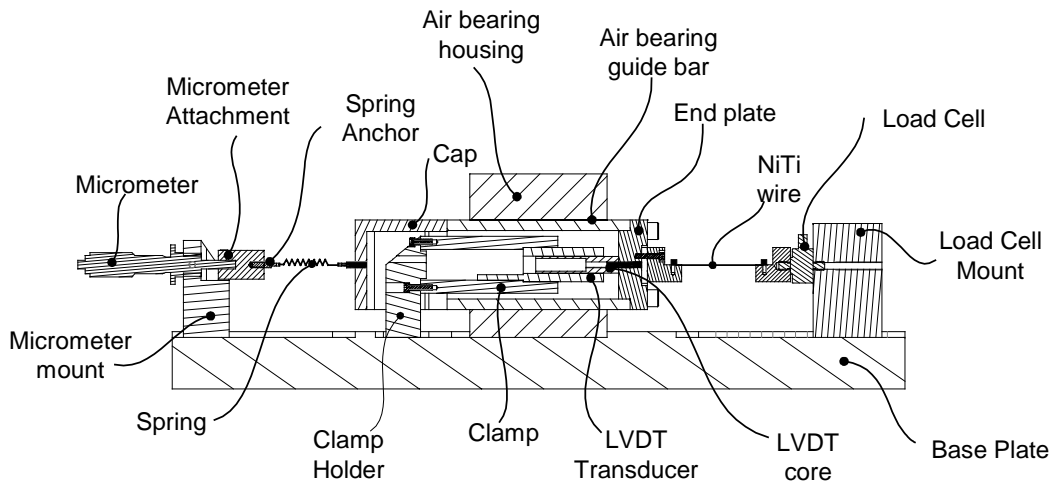


Fig 4: Cross-sectional View of Instrument

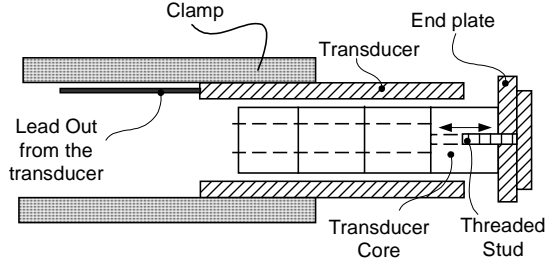


Fig 5: LVDT Setup

Control and Data Acquisition System

A block diagram of the approach to controlling and acquiring data is shown in Fig.6. The data acquisition system is based on a DaqBoard-2001™ by IOtech Inc. hosted in a generic personal computer. The DaqBoard-2001™ features a 200 kHz, 16 Bit A/D converter that is used to sample values from the load cell, LVDT, current meter and the voltmeter.

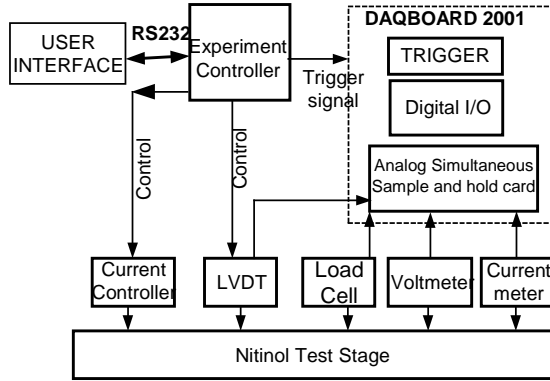


Fig 6: Block Diagram of Electrical Setup

A 4-channel simultaneous sample and hold card is used to sample the four analog signals simultaneously with the single A/D converter. A non-contact commercial current meter by F.W.Bell is used to measure the current running through the SMA wire sample. The mA-2000™ measures currents with a resolution of 0.1mA and an accuracy of 1% of the reading. A universal in-line amplifier conditions the signal from the load cell before being input into the DaqBoard-2001™. The voltage data combined with the current data will allow future studies of the variation in the resistance of shape memory alloys.

The Flexinol™ wire samples are driven by a commercial PWM power supply with

variable voltage settings and variable current limitation allowing the freedom of adjusting arbitrary voltages. A trigger signal is generated by the experiment controller and received by the DaqBoard-2001™ to control start time of acquisition. The experiment controller is a micro controller based unit that communicates with a RS232 serial port on a PC. The experiment controller allows the user to set a number of experimental parameters such as the number of actuation cycles, the duration of actuation, and the cooling time between actuation cycles.

Error Analysis

In analyzing the errors within the instrument, one should consider the following error sources that affect the force or displacement measurements.

Thermal Expansion

Fig 7 illustrates the effect of thermal expansion in the instrument as a result of temperature fluctuation in the surrounding environment. One way to minimize this effect in the instrument is to match the axial expansion of the guide bar with that of the base plate.

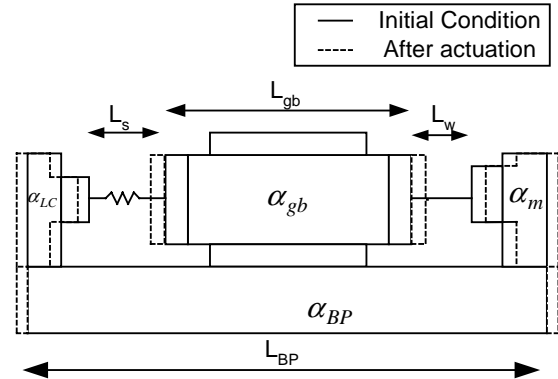


Fig 7: Thermal Expansion of Instrument

The axial expansion of the base plate, δ_{BP} , with a coefficient of thermal expansion, α_{BP} , length, L_{BP} , and a temperature fluctuation of, ΔT , is given in Eq (6).

$$\delta_{BP} = \alpha_{BP} L_{BP} \Delta T \quad (6)$$

Similarly, the axial expansion in the guide bar material, δ_{gb} , with a coefficient of thermal

expansion, α_{gb} , length, L_{gb} and a temperature fluctuation of, ΔT is given in Eq. (7).

$$\delta_{gb} = \alpha_{gb} L_{gb} \Delta T \quad (7)$$

Since the lengths of the spring, L_s and the NiTi wire, L_w should be constant, the uncertainty [6] in the force measurement, U_F , that results from expansion is a function of, k_s , α_{BP} , α_{gb} , L_{BP} , L_{gb} and ΔT , and is given in Eq.(8).

$$U_F = k_s \Delta T (\alpha_{BP} L_{BP} - \alpha_{gb} L_{gb}) \quad (8)$$

To minimize U_F , the expression parentheses should be nearly zero. Therefore, the ratio of the CTEs should be nearly equal to the ratio of the lengths as given in Eq (9). The guide bar is made of aluminum ($\alpha_{gb} \approx 23 \times 10^{-6}$ 1/°C), and the base plate can be made of CI-30 cast iron ($\alpha_{BP} \approx 10.5 \times 10^{-6}$ 1/°C). The appropriate length of the base plate that minimizes U_F is then about 400 mm.

$$\alpha_{BP} / \alpha_{gb} = L_{gb} / L_{BP} \quad (9)$$

Compliance of the Instrument

Compliance in structural components like the base plate, the load cell mount and the micrometer mount affect the uncertainty in displacement measurements. These parts need to be stiff to reduce the deflections and changes in geometry due to forces. The deformation in the geometry of the instrument is illustrated in Fig

8.

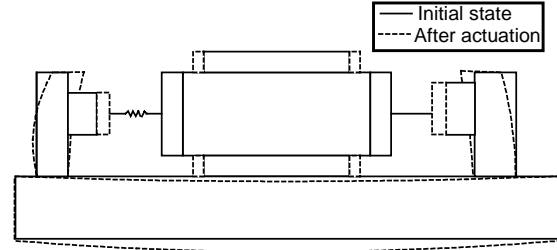


Fig 8: Deformation Due to Compliant Instrument

Fig. 10 illustrates the instrument as a combination of a mass and springs in series, whose stiffness can be predicted using finite element analyses. If the stiffness for each structural component, k_i , is combined using Eq (10), then the equivalent instrument stiffness, k_I , can be used in the simplified model of Fig. 9.

$$k_I = \left[\sum_{i=1}^n (1/k_i) \right]^{-1} \quad (10)$$

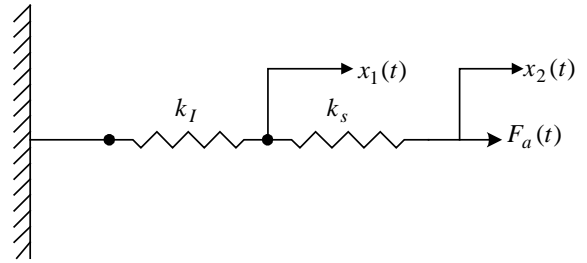


Fig 9: Integrated Spring Model

The uncertainty in the displacement measurement, U_c , is approximately the ratio of the actuator force, F_a , and the instrument stiffness, k_i , given in Eq (11)

$$U_c = F_a / k_i \quad (11)$$

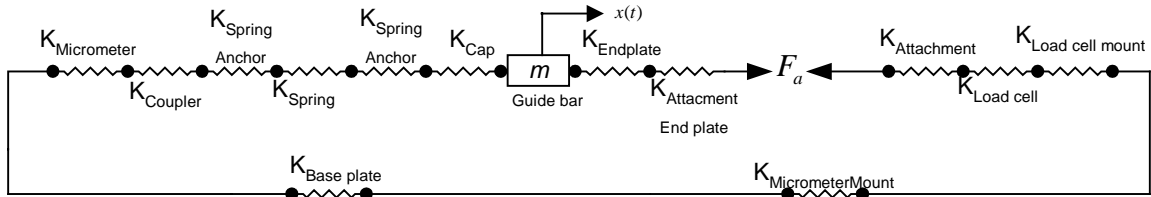


Fig. 10: Closed-loop Spring Model

Conclusion and Future Work

This paper describes the conceptual design, detailed design, and some error sources in a new instrument for characterizing Flexinol wires. The instrument uses a damped spring-mass system with an LVDT and force gage. A controller and data acquisition system enable force, displacement, current, and voltage to be measured as functions of time. Future experiments will characterize the variability in wire and actuator parameters, degradation of wire properties over many cycles, and optimization of control strategies.

Initially, the instrument will be used for investigating the transient displacement, steady-state actuation displacement, x_a , and actuation force, ${}^{ss}F_a$. Future work is necessary to characterize the transient actuation force produced by the wire. During the transient periods, the force recorded by the load cell is actually a combination of the wire's actuation force, the viscous damping forces, and inertial forces. Furthermore, the displacement of the mass is the convolution of the actuation force and the system's impulse response function. A method should be developed for separating these forces so that the transient actuation forces, ${}^cF_a(t)$ and ${}^eF_a(t)$ are obtained.

References

- [1] Darel E. Hodgson, Shape Memory Applications Inc., Ming H.Wu, Memry Technologies, and Robert J.Biermann, Harrison Alloys, Inc. "Shape Memory Alloys.
- [2] John A.Shaw and Stelios Kyraiakides, "Thermomechanical Aspects of NiTi", *Journal of Mech.Phys Solids*, Volume 43 No.8, pp.1243-1281, 1995.
- [3] C.Liang, C.A.Rogers, "Design of Shape Memory Alloy Actuators", *Journal of Mechanical Design*, June 1992, Vol.114/223
- [4] "Precision Machine Design" Slocum, A.. *Prentice Hall. Englewood Cliffs, New Jersey. 1992*
- [5] Dynalloy Inc.,Costa Mesa, CA, "Material properties of Flexinol".
- [6] "Test Uncertainty-Instruments and Apparatus", *ASME PTC 19.1.1988, American Society of Mechanical Engineers, 1998.*